

Calorimetric Method To Determine Self-Accelerating Polymerization Temperature (SAPT) for Monomer Transportation Regulation: A Heat Balance Approach

Min Sheng,*^{†,‡} Florin Dan,[‡] Steve Horsch,[§] Robert Bellair,[§] Marabeth Holsinger,[†] Travis Scholtz,[†] Stephan Weinberg,^{||} and Alan Sopchik^{†,‡}

[†]Reactive Chemicals, The Dow Chemical Company, Midland, Michigan 48667, United States

[‡]Analytical Sciences, The Dow Chemical Company, Midland, Michigan 48667, United States

[§]Reactive Chemicals, The Dow Chemical Company, Freeport, Texas 77566, United States

^{||}PM Tech Center Methacrylates, The Dow Chemical Company, Deer Park, Texas 77536, United States

^{†,‡}Process Dev & Optimization, The Dow Chemical Company, Deer Park, Texas 77536, United States

ABSTRACT: In our previous paper, kinetic parameters for the thermal polymerization of methyl methacrylate (MMA) inhibited with 4-methoxyphenol (MEHQ) were determined by isothermal and nonisothermal calorimetric tests. In this paper, the Self-Accelerating Polymerization Temperature (SAPT) was determined based on the heat balance using measured or estimated heat transfer coefficients and the aforementioned kinetic parameters. Herein both the PIT approach and heat balance approach are validated for MMA inhibited with MEHQ in a 1 gallon container, at conditions where the monomer in the container self-increases its temperature from 2 °C lower to 6 °C higher than the environmental temperature in a period of 7 days (H1 method). Various experimental and computational methods for determining the heat transfer coefficients for these tests are described. A screening method for SAPT based on PIT (Polymerization Induction Time) was proposed, as follows: for monomers having a well-defined PIT at 75 °C greater than 7 days with the max heat generation rate much lower than 120 μW/g, their SAPT can be reported as >75 °C. Otherwise, additional testing is needed and SAPT can be estimated based on either the PIT approach or heat balance approach.

KEYWORDS: monomer, self-accelerating polymerization temperature (SAPT), calorimetric method, overall heat transfer coefficient, heat balance

1. INTRODUCTION

The United Nations Recommendations on the Transport of Dangerous Goods, Model Regulations, Rev.19 (2015)¹ states that the Self-Accelerating Polymerization Temperature (SAPT) shall be determined in accordance with the test procedures established for the Self Accelerating Decomposition Temperature (SADT) for self-reactive substances. There are four recommended test methods for SADT determination, H1 to H4, which differ in their measurement techniques.^{2–4} Generally, reaction kinetic parameters are obtained by testing a relatively small quantity of chemicals with adiabatic (H2), isothermal (H3), or other calorimeters. Heat loss per unit of substance in the desired package is needed for heat balance evaluation to determine SADT or SAPT. As UN “Manual of Tests and Criteria” suggests,² the heat loss per unit of substance in a package should be determined by calculation or by measuring the half-time of cooling test with the substance of interest or another substance having similar physical properties. Due to the cost of running a cooling test in a large package, the calculation approach is often more practical. Knowledge of the quantity of material, dimensions of the package, heat transfer in the substance, and the heat transfer through the packaging to the environment need to be accounted for to ensure accurate results. Researchers^{3,5–7} commonly evaluate the SADT by applying the overall heat

transfer coefficient (*U* value) of 11.3 W/m²·K (2.0 Btu/h·ft²·°F), which is considered as the outside surface heat transfer coefficient.^{8–10} For a small vessel, this simplification is valid since the internal thermal resistance is relatively small compared to the external thermal resistance. However, for a large vessel, the internal thermal resistance becomes significant and the overall heat transfer coefficient will be lower than the surface heat transfer coefficient. Water cooling measurements in ref 11 indicates that the *U* value of a 55 gallon steel drum and 5000 gallon tank trunk with water is 25% lower and 40% lower, respectively (Table 1). The application of a *U* value of 11.3 W/m²·K to those vessels could result in a false SADT/SAPT value (SAPT > 75 °C), since it assumes greater heat removal than realistic.

Even for packages having the same dimensions but filled with different substances, the *U* value may vary because the physical properties of the substances may significantly change the internal thermal resistance within the package, especially for a large static package. When a transportation vessel is moving on the road, the vibration and mixing of the liquid reduces the internal thermal resistance. As such, for SAPT values lower than but close to 75 °C one could consider

Received: January 8, 2019

Published: April 18, 2019



Table 1. Measured Overall Heat Transfer Coefficient of Transportation Package in References¹¹

Vessel	Testing substance	Mass (kg)	<i>U</i> value (W/m ² ·K)
Round-bottom glass flask	water	1	12
55 gallon steel drum	water	220	8.5
5000 gallon tank truck	water	19 700	6.8
Insulated storage tank	water	42 700	2.7
Insulated railcar	water	76 000	1.0

including the mixing effect into the calculation of the overall heat transfer coefficient, but experiments would likely be necessary to validate assumptions. However, when a large vessel is at rest, the heat inside the vessel is only transferred out by conduction through bulk liquid and natural convection caused by a temperature gradient.^{8,12} The heat transfer capability of material in a large static vessel is relatively small and will dominate the overall heat transfer coefficient. Furthermore, the thermal conductivity, thermal expansion, and viscosity of the liquid may also play a significant role in the overall heat transfer coefficient by reducing either the heat conduction or natural convection.⁸ For example, the internal thermal resistance for samples of viscous liquids, pastes, and solids is so high that neither the Semenov model with overall heat transfer coefficient nor the Dewar method (H4) should be used for SADT/SAPT determination.^{13,14}

During a polymerization reaction, the monomer substance transforms from a liquid into a viscous liquid and then into a polymeric solid at a high conversion. This introduces a challenge to calculate the *U* value for SAPT purposes. An assumption has to be made that the polymerization conversion is still low when the temperature of the monomer in a desired package reaches 6 °C higher than the environmental temperature, so that the physical properties and *U* value remain unchanged. With this assumption, the *U* value can be determined by performing a cooling test with unreacted monomer liquid in the desired container. The assumption is valid for many monomers owing to the rate of polymerization once initiated and the amount of energy associated with polymerization.¹⁵

In our previous paper (Part I), the PIT and kinetic parameters for methyl methacrylate (MMA) inhibited with 4-methoxyphenol (MEHQ) were determined with isothermal calorimetric tests. In this report (Part II), the overall heat transfer coefficients of different chemicals were experimentally determined in a 1 gallon drum by measuring their cooling profiles. Within the same container, an H1 test with MMA monomer was conducted to verify the SAPT result based on the heat balance calculation with the previously evaluated kinetic parameters.

2. EXPERIMENTAL PROCEDURES

2.1. Heat Transfer Coefficient Measurement for 1 Gallon Drum.

Chemicals used in this study include methyl methacrylate, MMA (Aldrich 99%), with less than 30 ppm MEHQ and dimethyl phthalate, DMP (Aldrich 99%). GC analysis indicated the MEHQ level in the MMA sample was 25 ppm. The 1 gallon steel drums used in this study have a UN rating code of 1A1/1.5/250/16/USA. They are 17 cm in diameter, 22 cm in height, 0.9 mm in wall thickness, 0.831 kg in weight, and 3.88 L of internal volume, Figure 1a.



Figure 1. Photos of 1 gallon drum used in this study: (a) new drum; (b) drum after MMA H1 test; and (c) the bottom of drum after MMA H1 test.

To measure the overall heat transfer coefficients of water, DMP, and MMA, a fill volume of 3.49 L was used. Typically, for a given test, 3.49 L of the appropriate chemical were loaded into the aforementioned 1 gallon vessel and the system was placed in an oven. Once the sample temperature reached the desired set point, the drum was taken out from the oven and set on a wood block at ambient conditions to cool. The temperature profiles of the sample and the surroundings were monitored over the entire process. The thermocouple for the sample was placed at the center of the drum.

2.2. H1 Test for MMA in 1 Gallon Drum. A conduction oven was used for H1 tests of MMA inhibited with 25 ppm MEHQ. For safety reasons, this oven was located in a Bunker and monitored remotely. The oven was preheated to a desired temperature, and then a drum with 3.49 L of MMA sample (90% filling level) was transferred into the oven. Two thermocouples were installed on the drum with Swagelok fittings to monitor the sample temperature. For the first H1 test (oven temperature: 76 °C), one thermocouple was placed at the center of the monomer liquid and the other one next to the inside wall of the drum. For the second H1 test (oven temperature: 72.2 °C), one thermocouple was still placed at the middle height of the axis but the other one at the top surface of the liquid in the drum. An additional thermocouple for the oven temperature was employed for both H1 tests.

A venting line was also installed on the drum for pressure measurement. However, it was found that MMA condensed and polymerized in the line, so pressure data were not accurately recorded. The SADT tests resulted in a high internal pressure during the polymerization reaction of bulk MMA and bulged the drum. Figure 1b and c show an example of the bulging top and bottom of a drum after being used for MMA H1 testing.

3. RESULTS AND DISCUSSION

3.1. Heat Transfer Coefficient. **3.1.1. Experimental Measurement with 1 Gallon Drum.** The overall heat transfer coefficient (*U*) can be estimated directly from measurement of the temperature–time profile during cooling of a heated vessel.

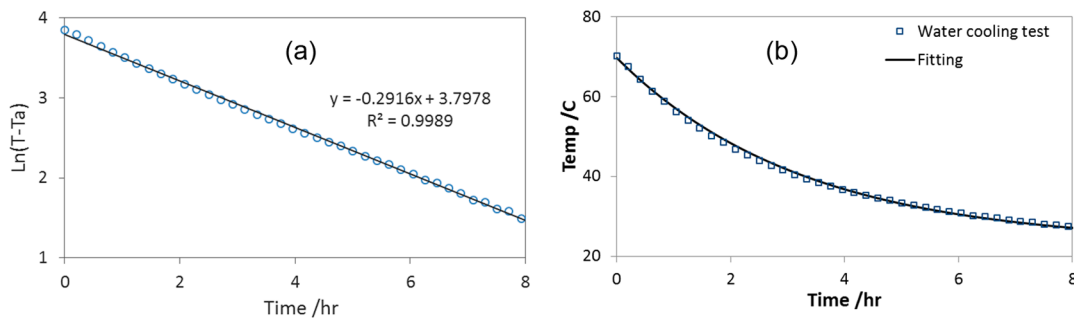


Figure 2. Data fitting for water cooling test (a) using the half-time of cooling method; (b) nonlinear regression.

Ideally, the U of a given system should be measured to give the most accurate predictions of SAPT. However, this is not always feasible for large vessels/packages, and it can be time and resource intensive. When feasible, the UN “Manual of Tests and Criteria”² recommends use of the half-time of cooling method, where a linear relationship can be found as eq 1.

$$\ln(T - T_a) = \ln(T_{0i} - T_a) - \frac{UA}{mC_p}t \quad (1)$$

Figure 2a shows the fit for the linear regression of the above equation, whose slope was used to estimate the heat transfer coefficient for multiple chemicals in this container.

An alternative method to determine the U value from test data is via nonlinear regression of the heat transfer equation (eq 2), wherein the temperature profile can be fitted by applying the fourth-order Runge–Kutta method¹⁶ and minimizing the mean square error to solve for the U value. Figure 2b gives an example of this approach.

$$mC_p \frac{dT}{dt} = UA(T - T_a) \quad (2)$$

One advantage of the nonlinear regression approach over the half-time of cooling method is that it also can be applied to the heating portion of the temperature profile, as shown in Figure 3. Normally, use of the heating profile is not recommended for estimation of the U value because it is challenging to maintain the temperature of the oven atmosphere at a constant value. However, the heating profile of the unreacted monomer in a desired drum is available during an H1 test if a cold drum is transferred into a hot oven. Therefore, this heating profile and nonlinear regression

approach is helpful to confirm the U value of each H1 test with that from the cooling test.

The measured U values for 1 gallon drums loaded with water, DMP, and MMA, respectively, are listed in Table 2.

Table 2. Overall Heat Transfer Coefficient (U , W/m²·K) of a 1 Gallon Drum with Different Chemicals

	Cooling test measurement ^a	Film heat transfer coefficient	CFD unsteady state simulation	CFD steady state simulation
Water	11.8	10.8	6.6	12.7
DMP	7.4	9.7	4.0	6.5
MMA	9.0	10.4	5.1	9.8

^aUncertainty of measurement is approximately 10%.

Previously published studies for SADT of organic materials in drums have used a U value of 11.3 W/m²·K.^{3,5–7} The measured U value for water is close to that value. However, the measured U values of MMA and DMP are smaller than the literature value, even for such a small drum, which means the application of this literature value for the SADT estimation of those chemicals is not conservative.

3.1.2. Heat Transfer Coefficient Estimation. For the three tested chemicals, it can be assumed that the heat transfer characteristics of the drum wall and outside the drum are identical, but the heat transfer characteristics inside the drum are different due to different physical properties. For such a storage vessel, the heat transfer inside the drum is primarily due to either heat conduction or natural convection. Heat conduction depends on thermal conductivity, and natural convection mainly relates to thermal expansion and viscosity of the fluid. As can be seen from the difference of measured U values, thermal conductivity, thermal expansion, and viscosity of the chemical (Table 3) in the same drum can have a significant effect on the overall heat transfer coefficient. A good estimation method should include these properties in the calculations.

3.1.2.1. Film Heat Transfer Coefficient. The film coefficient is widely used to estimate the heat transfer coefficient of a fluid due to natural convection. The following isothermal surface vertical cylinder model is used to estimate the U value:¹⁷

$$\text{Film coefficients: } \frac{hD}{k} = 0.59(Gr \cdot Pr)^{0.25} \quad (3)$$

$$\text{where } Pr = \frac{C_p \mu}{k} \text{ and } Gr = \frac{g \rho^2 \beta (T_w - T_a) D^3}{\mu^2}.$$

This model tends to underestimate the outside surface heat transfer coefficient between the vessel wall and ambient air. Hence, the outside surface heat transfer coefficient of 11.3 W/

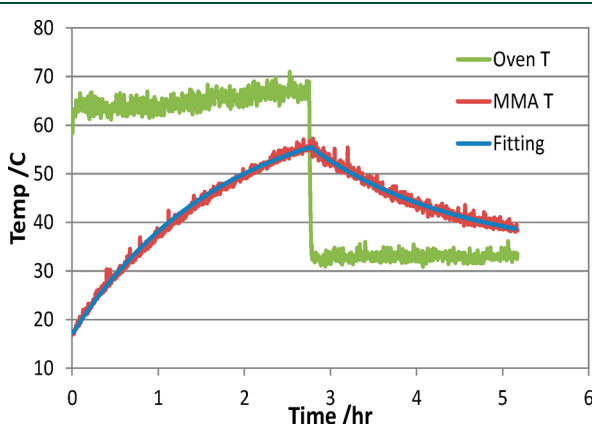


Figure 3. Nonlinear regression for both heating temperature profile and cooling temperature profile.

Table 3. Physical Properties of Chemicals at 50°C

	Density, ρ (kg/m ³)	Heat capacity, C_p (J/g·K)	Thermal conductivity, k (W/m·K)	Viscosity, μ (N·s/m ²)	Coefficient of thermal expansion, β (1/K)
Water	984.448	4.178	0.6374	5.60×10^{-04}	5.696×10^{-04}
DMP	1165.42	1.606	0.1463	5.45×10^{-03}	8.368×10^{-04}
MMA	908.59	1.791	0.1358	4.35×10^{-04}	1.319×10^{-03}

m²·K is employed^{8,9} and the film coefficient model is only applied for the liquid side of the vessel wall.

$$\text{Overall heat transfer coefficient: } U_o = \frac{1}{\frac{1}{h_o} + \frac{(r_o - r_i)A_o}{kA_{lm}} + \frac{A_o}{A_i h_i}} \quad (4)$$

$$\text{where } A_{lm} = \frac{A_o - A_i}{\ln(A_o/A_i)}.$$

All physical properties of water, DMP, and MMA at 50 °C, which is the average temperature of the cooling test, are obtained from the DIPPR physical property database¹⁸ (Table 3). Since the surface temperature is unknown at the beginning of the calculation, a trial-and-error method is needed to solve the equations. The results of this film coefficient method for estimating the U value are tabulated alongside the measured heat transfer coefficients in Table 2. Compared with the measured values, this engineering estimation method results in U values that are larger or smaller than the measured values depending on the material.

3.1.2.2. Unsteady State CFD Simulation of a Cooling Test. Another approach to estimate the U value is by simulating the heat transfer phenomena of a heat exchange process, such as a cooling test, via CFD modeling (ANSYS).^{10,19} As shown in Figure 4, a 2-D axisymmetric finite element model was built for

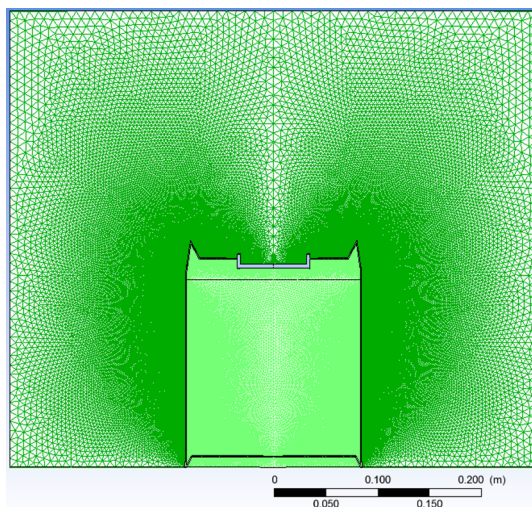


Figure 4. 2-D axisymmetric finite element model for 1 gallon drum.

the 1 gallon drum enclosed in a cylinder space. The drum in Figure 4 had a diameter of 17 cm and a height of 22 cm, the same dimensions of 1 gallon drum used in H1 test, while the enclosed space had a diameter of 51 cm and a height of 44 cm. There were two fluid domains inside the drum: air headspace and liquid, i.e. the inhibited monomer. The initial temperature of the drum (and the fluids within it) was set at 70 °C. The vertical walls and top were set at 20 °C with a constant temperature boundary condition and the bottom of the enclosed space with a nonheat flux boundary condition. CFD code was used to simulate the unsteady state cooling process of

this hot drum with hot fluids in a cold enclosure. Constant physical properties (50 °C, Table 3) were used for the simulation. The “PISO” scheme was used for pressure–velocity coupling, and “PRESTO!”, for pressure. The time step was set as 30 s with 500 iterations for each time step (details in Appendix 1).

With the unsteady state CFD simulation, the cooling profile of location B (shown in Figure 5) was obtained. Then the nonlinear regression was applied to extract the U value from the cooling profile. The results of this approach to estimate the U value of three chemicals in a 1 gallon drum are also listed in Table 2. Compared to measurement results, unsteady state CFD simulation underestimates the U values. This may be caused by the accumulation of a small truncation error which happened at each time step. Increasing the number of iterations for each time step may reduce this error, but this would require intensive computational resources.

An example of temperature contour and velocity vector from the cooling simulation is presented in Figure 5 (water cooling simulation at time of 67 min). For such a cooling test, the substance within the thin liquid film next to the drum wall is cooled by air outside of the drum. The low temperature in this film results in a relatively high density, and the gravity causes a downward liquid movement. As shown in Figure 5b, the downward liquid film movement has a significantly higher velocity than the upward velocity of bulk liquid. This downward movement brings cold liquid to the bottom of the drum and continuously pushes the cold liquid to the center of the bottom. Then, a small upward liquid movement is established in the bulk liquid due to the continuity of the liquid phase. With the horizontal heat transfer through the film, the upward liquid movement establishes a vertical temperature profile within the bulk liquid, as shown in Figure 5a. The vertical temperature profile is plotted in Figure 6a, along the axis crossing all domains.

To confirm the vertical temperature gradient within the liquid, an additional water cooling test was carried out, by directly adding hot water into a 1 gallon drum (no heating portion) and recording the cooling curves at different locations (A to E in Figure 5). Since the drum was cold before the hot water was added, the temperatures of C and D points were slightly lower at the beginning. After the initiation period, the temperatures followed the order C > B > D > A > E, as shown in Figure 6b. By comparing the temperatures in Figure 6a and temperatures at 37 min in Figure 6b, the temperature distribution of unsteady state CFD simulation at 67 min approximately corresponds to the temperature distribution of the actual cooling test at 37 min. The cooling rate in the CFD simulation is much slower than that of a real test, but the vertical temperature distribution within liquid agrees well.

Since a max temperature difference of 4.8 °C between A and B was observed during the water cooling test in such a small vessel, a significantly higher temperature difference between the bottom and the middle of a static vessel can be achieved for a large vessel. Ferguson¹¹ observed a 20 °C temperature difference from the bottom to the center of a horizontal

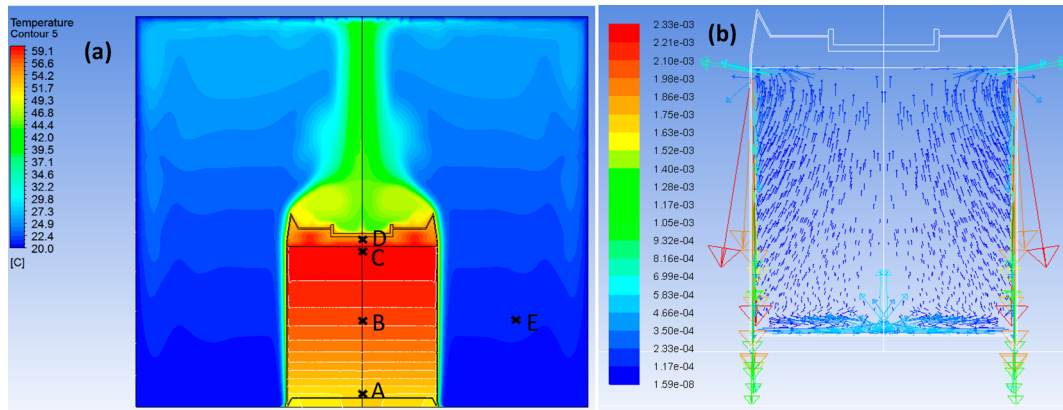


Figure 5. (a) Temperature contour and (b) liquid velocity vectors colored by velocity magnitude (m/s) for water cooling simulation at time = 67 min. A, B, C, D, and E represent the following spatial positions: A ($R = 0 \text{ mm}$; $H = 15 \text{ mm}$), B ($R = 0 \text{ mm}$; $H = 96 \text{ mm}$), C ($R = 0 \text{ mm}$; $H = 176 \text{ mm}$), D ($R = 0 \text{ mm}$; $H = 188 \text{ mm}$), and E ($R = 170 \text{ mm}$; $H = 96 \text{ mm}$).

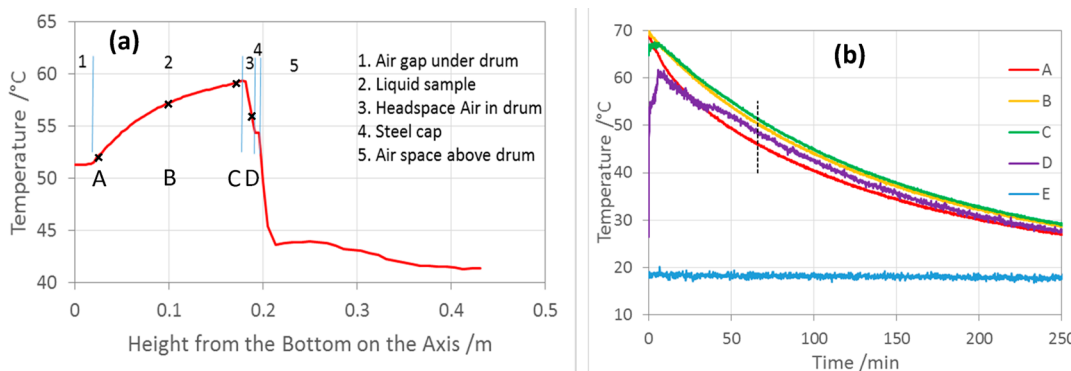


Figure 6. Temperature of different locations on the axis. (a) CFD simulation at 67 min (Figure 5); (b) experimental water cooling test. Data labeled as A, B, C, and D represent the temperature at the positions defined in Figure 5.

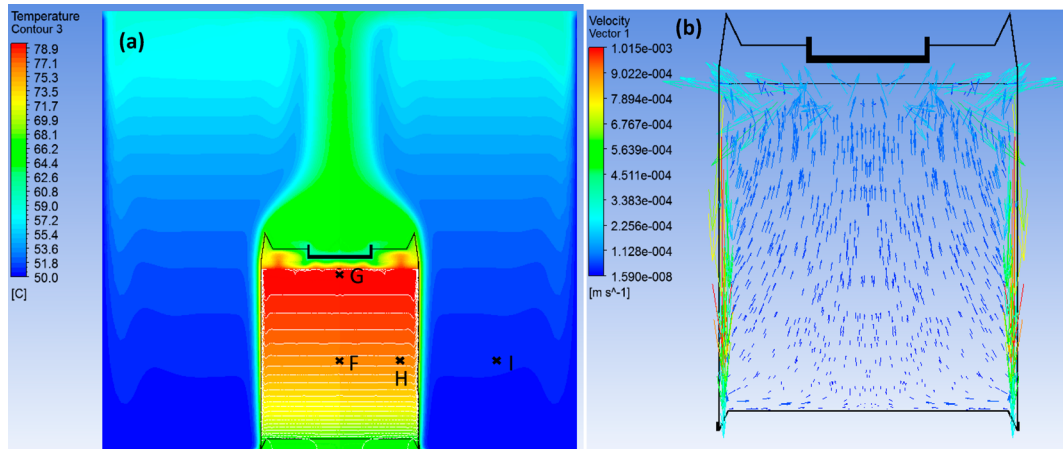


Figure 7. Temperature contours of the drum with MMA sample with a steady state simulation. F, H, I, and G represent the following spatial positions: F ($R = 0 \text{ mm}$; $H = 96 \text{ mm}$), H ($R = 70 \text{ mm}$; $H = 96 \text{ mm}$), I ($R = 170 \text{ mm}$; $H = 96 \text{ mm}$), and G ($R = 0 \text{ mm}$; $H = 176 \text{ mm}$).

cylinder-shape railcar in a water cooling test. For this reason, to accurately monitor the temperature of a static storage vessel or a static transportation tank, one should avoid taking measurements at the bottom of the tank.

3.1.2.3. Steady State CFD Simulation of Constant Heat Generation. Another alternative approach to estimate the U value by applying CFD code is to simulate a steady state heat transfer process.^{20,21} This approach can reduce the truncation error by increasing the calculation iterations and avoid the

error accumulation observed in unsteady state simulation. The same finite element model (Figure 4) was used for this approach. The vertical wall of the enclosure space was set at 50°C with a constant temperature boundary condition, while the top and bottom were set as a nonheat flux boundary condition. The liquid domain inside the drum was assigned an artificial constant volumetric heat generation rate of 7000 W/m^3 , which enabled the heat to transfer from the liquid inside the drum to the enclosure. In order to reduce the effect of mesh size on

surface heat convection,²² boundary adaption and gradient adaption were applied in the simulation (details in Appendix II). Temperature dependent physical properties of the heat exchange medium (both fluids and steel; an example shown in Appendix III) were used since a higher error of U value was reported²³ by using constant physical properties.

The steady state simulation was performed to obtain the heat transfer due to temperature gradient caused by the heat generated from the chemicals and the mass transfer due to natural convection. With the average temperature of the liquid domain, the U value is calculated with eq 5.

$$U = \frac{Q}{A(T_{av} - T_a)} \quad (5)$$

The results of this approach for estimating the U value of MMA are listed in Table 2. Compared with the measured value, steady state CFD simulation gives U values with an error of $\pm 15\%$; thus, it is the recommended method to estimate the heat transfer coefficient.

An example of temperature distribution and velocity vector (MMA as liquid) is presented in Figure 7. Similar to unsteady state simulation of the cooling test, the substance in the thin liquid film next to the drum wall in this steady state simulation is cooled by air outside of the drum and forms a downward liquid movement. However, the constant internal heat generation contributes to the upward liquid movement in the bulk liquid by increasing the vertical temperature gradient. Most of the cooled liquid escapes from the cold film along the downward movement, so that the velocity in the film decreases remarkably and thus little cold liquid reaches the bottom of the vessel. Based on the CFD simulation, the horizontal liquid movement at the bottom of the vessel for this steady state simulation of constant heat generation is much smaller than that for the unsteady state simulation of a cooling test.

An example of horizontal temperature distribution is plotted against the radius along the line of F–H–I in Figure 7 and illustrated in Figure 8. The vertical temperature gradient is

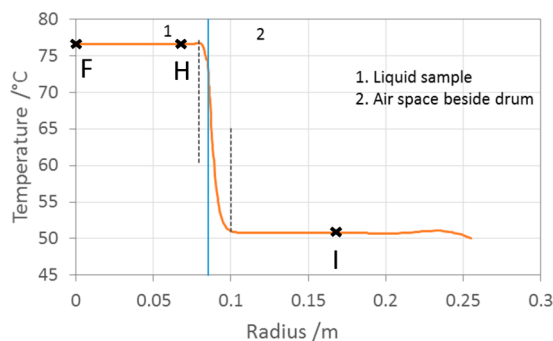


Figure 8. Horizontal temperature distribution along line of FHI (Figure 7). Data labeled as F, H, and I represent the temperature at the positions defined in Figure 7.

significant within the liquid, but the horizontal temperature gradient is very small in the bulk liquid, except in the thin liquid film. Since the temperature gradient primarily exists within the thin films on both sides of the drum wall, thermal resistance of both films dominates the overall heat transfer phenomena. This supports the approach to estimate the overall heat transfer coefficient with a film heat transfer coefficient.

For the MMA H1 tests conducted within a 1 gallon drum, two thermocouples were installed in the drum to measure the

internal temperatures. The first H1 test, at 76 °C, had them located at positions of F and H, respectively (as shown in Figure 7), to measure the horizontal temperature difference during the entire test. The second H1 test, at 72.2 °C, had them placed at the F and G position, respectively, to measure the vertical temperature difference during the polymerization reaction. As shown in Figure 9a, the horizontal temperature difference between the drum center (F) and its side (H) is almost negligible for the entire test, except for a short period between 91.5 and 93 h. The slight lower temperature at the side (H) during this short period likely may not be caused by the heat generation from the polymerization reaction but the lack of enough liquid movement from natural convection. After this period, both locations are under conditions close to the adiabatic condition and no liquid movement due to high molecular weight polymer formed, so that the temperature difference is negligible again. As shown in Figure 9b, the vertical temperature difference between the middle height (F) and the top (G) on the axis is significant when there is heat generation from the polymerization reaction. At the beginning of the reaction, the top temperature (G) is lower than the middle temperature (F), owing to little or no initial natural convection. Then, the top temperature becomes significantly higher from 155.2 to 155.7 h, with a maximum difference of 49 °C. This measured temperature difference supports the vertical temperature difference suggested by the steady state CFD simulation. Obviously, a large vertical temperature gradient results from a high reaction rate and thereby high heat generation rate. Meanwhile, the polymerization reaction turns the liquid monomer into a high molecular weight polymer and significantly increases the viscosity of the bulk material in the drum. The liquid movement is slowed down due to the high viscosity and eventually stopped at a high polymerization conversion. The heat convection contribution is completely removed from the heat transfer phenomena in the bulk material. Since the contents in the drum are still cooled by air on the top of the drum, the top temperature becomes lower from 155.7 h to the end of the reaction, with a maximum difference of 35 °C.

3.2. SAPT Determination Based on Heat Balance Approach. **3.2.1. H1 Test within a 1 Gallon Drum.** Two H1 tests were conducted using MMA inhibited with 25 ppm MEHQ; one was carried out at 76 °C and another one at 72.2 °C, respectively. The temperature–time profiles from both tests are presented in Figure 10. Although the oven temperature was not constant over the entire test, the first 4 h of heat-up data from the test was sufficiently constant to confirm the previously measured U value with the nonlinear regression method. Calculated U values from both tests agreed with the U value previously determined from the cooling profile within the uncertainty range. The induction time of the H1 test at 76 °C was lower than that of 72.2 °C, which is consistent with the result from isothermal micro calorimeter tests. The temperature profiles of the polymerization reaction were similar for both H1 tests. Due to the heat from the reaction, the oven temperature also increased with a max overheat of 20 °C occurring at the same time as the peak sample temperature. The time required for the sample temperature to increase from 2 °C lower to 6 °C higher than the oven temperature was 3.4 days for the 76 °C test and 6.1 days for the 72.2 °C H1 test, respectively. In order to achieve a 7-day period for this much temperature rise, the oven temperature should be set lower than 72.2 °C and the SAPT of

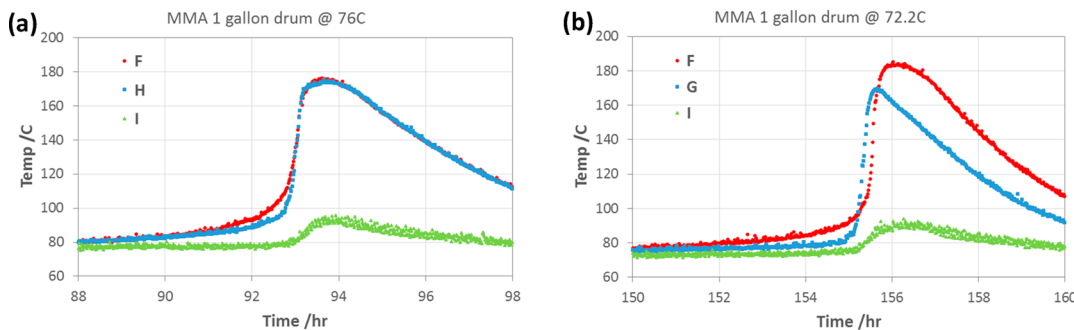


Figure 9. Measured temperature difference in H1 test. (a) Horizontal temperature contour; (b) vertical temperature contour. Data labeled as F, G, H, and I represent the temperature at the positions defined in Figure 7.

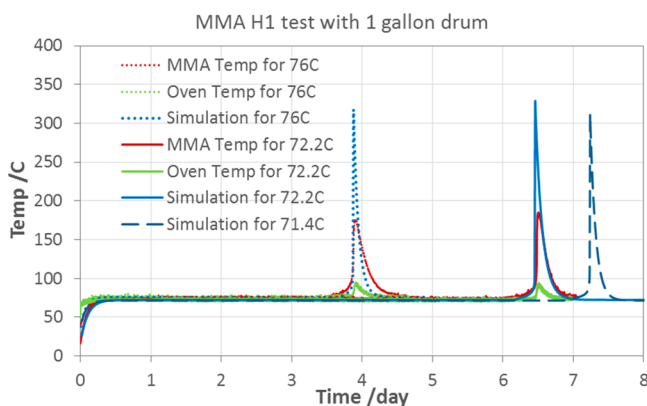


Figure 10. H1 test result with simulation based on kinetic model.

MMA in this drum should be slightly lower. Instead of repeating the test and tuning to the exact temperature, these two H1 tests were used to validate models and then simulation with the models was used for SAPT estimation. A summary of the results is listed in Table 4, and the SAPT found for this drum of MMA sample was 71.4 °C.

Table 4. Sensitivity of SAPT Estimation to U Value

Proposed U value for 1 gallon drum (W/m ² /K)	SAPT measurement (°C)	SAPT estimation (°C)		
		Semenov's model with ARC test (critical ambient temperature)	Simulation with full kinetics	PIT kinetics
0	—	—	71.1	71
3	—	65 (65)	71.2	71
6	—	75 (72)	71.3	71
9	<72.2	80 (77.5)	71.4	71
12	—	80 (78)	71.6	71

3.2.2. Heat Balance Simulation. The kinetic parameters from isothermal micro calorimetry (combined with filling level correction)¹⁵ and the measured U value for MMA in a 1 gallon drum were used to simulate the H1 tests, and the results are plotted in Figure 10. The following energy balance equation was used in the simulation:

$$-mC_p \frac{dT}{dt} = m_m \left(\Delta H_{r_z} \cdot \frac{d\alpha_{in}}{dt} + \Delta H_{r_m} \cdot \frac{d\alpha_M}{dt} \right) + UA(T - T_a) \quad (6)$$

The simulation predicts the early portion of the polymerization exotherms of both H1 tests quite well; however, it overpredicts

the peak sample temperature during the polymerization. The overprediction is expected because the monomer reached the “ceiling temperature” during the experiment and the model does not account for its impact on the heat of reaction. Specifically, the heat of reaction used in the model was estimated from isothermal calorimetry carried out below the “ceiling temperature” and represents the entire heat of polymerization. Importantly the experimental data and the model are in good agreement until the “ceiling temperature” is reached. Since runaway polymerization will occur well below the “ceiling temperature,” adding complexity to the model to account for the variability in the heat of reaction is not justified.

Utilizing the criteria of SADT, simulation can be used to determine the monomer SAPT, which is the lowest environmental temperature at which the temperature increase of a monomer in a specified package is at least 6 °C during a period of 7 days, starting from the time when the monomer temperature is 2 °C lower than the environmental temperature. Based on the simulation, the SAPT of the MMA monomer with 25 ppm MEHQ in a 1 gallon drum with 10% air headspace is 71.4 °C. The simulated temperature profile for an H1 test at 71.4 °C is presented in Figure 10 for illustrative purposes.

For the simulations shown in Figure 10, 3.9–5.6% of MMA conversion is required to achieve a 6 °C temperature rise. If the monomer is transported in a larger vessel, the heat removal rate will be smaller and more energy will be available in the reaction mass to raise the temperature by 6 °C (i.e., less conversion required to achieve the temperature rise). Therefore, the assumption that the monomer’s physical properties can be utilized to estimate the overall heat transfer coefficient, density, and velocity profiles is valid.

It is important to remember that, just like SADT, the SAPT is not a constant parameter for any given monomer. Rather, it is dependent on the monomer properties, inhibitor levels, available oxygen, and the packaging properties as well as environment. If different sizes of package are used to ship the same monomer, the SAPT will vary because of the change in heat loss per unit of monomer mass. The impact on SAPT to changes in heat transfer will be a function of the initial polymerization rate. By varying the U value in the simulation of MMA in the 1 gallon drum, the sensitivity of SAPT to package size in this system can be seen. It was found that, for MMA, the SAPT only decreases from 71.6 to 71.1 °C when the U value changes from 12 W/m²/K to 0 W/m²/K (adiabatic) (Table 4). Out of the required 7 days of the H1 test at 71.4 °C, the induction time lasts 6.7 days (96%). Since there is almost no

heat generation from the sample during the induction time, the decrease of U value will not impact the sample temperature. Thus, only 4% out of the required 7 days is impacted by the heat loss. Therefore, it can be concluded that the SAPT of this monomer is primarily governed by PIT in typical shipping containers because of their limited ability to allow heat to escape.

If only PIT kinetics are used to determine the SAPT of MMA in this drum, the result is more conservative because the heat generation over PIT is insignificant and the ending temperature will be less than 6 °C higher. As listed in Table 4, SAPT from the PIT equation is lower than the SAPT from simulation with full kinetics. Also, the SAPT from PIT is not dependent on the U value or package size at all for systems where no heat is generated during the induction phase. The advantage of this PIT approach for SAPT is that it can avoid the kinetic fitting, measurement of U value, and complex simulation.

3.2.3. Semenov's Model with ARC Test. As suggested in H2 and H3 test methods by the "Manual of Tests and Criteria",² the Semenov model evaluates the heat balance based on the heat generation measured by calorimeters and the external heat loss of the transportation vessel. This model has been used to calculate SAPT for monomers.^{24,25} However, we found out that the SAPT determined based on this model with the ARC test result is not conservative.

The Semenov model for MMA in a 1 gallon drum is presented in Figure 11. The adiabatic heat generation rate was

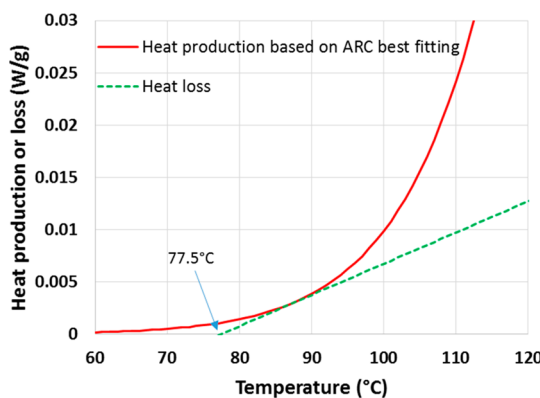


Figure 11. Semenov model for 1 gallon drum H1 test: heat production curve based on the best fitting of the ARC in our previous paper; heat loss curve based on measured U value.

obtained from kinetic parameters of the ARC best fitting, shown in our previous paper. It is challenging to obtain detailed multiple mechanism kinetic information from ARC data, while the best fitting of ARC data with a single mechanism is often employed to obtain the kinetic parameters. The heat loss rate was calculated based on the measured overall heat transfer coefficient (U) of a 1 gallon drum with the MMA sample. The heat loss curves were tangent to the adiabatic heat generation curve at the temperature 87 °C with a critical ambient temperature of 77.5 °C, which resulted in a SAPT of 80 °C. Since these temperatures were much lower than the detected onset temperature by ARC (113 °C), the self-heat rate and reaction kinetics at these temperatures were not directly measured by ARC. The heat production was predicted with the assumption that the reaction mechanism at low temperature was the same as that after the onset

temperature. For inhibited monomers, this assumption might not be valid since unstable MMA with MEHQ in a storage vessel undergoes a multiple mechanism reaction, including induction, bulk polymerization, and polymerization suppression behavior above ceiling temperature.²⁶ The induction reaction normally dominates at low temperature, but its reaction rate is not defined in the ARC test. Also, this approach was not conservative because the ARC test could miss other kinetic information as well, such as the autocatalytic process in the MMA polymerization reaction. Based on the Semenov model with ARC data, the SAPT for MMA in the tested drum is determined as 80 °C, which means it is safe to hold it at 80 °C with a max temperature of 86 °C at the end of 7 days. Obviously, this does not agree with two actual H1 drum tests, where a runaway polymerization was observed in shorter periods and at lower temperatures, 3.4 days at 76 °C and 6.1 days at 72.2 °C.

3.2.4. Friedman Differential Isoconversional Model. In a recent paper, Roduit et al.²⁷ presented the basic principles of a new kinetic analysis workflow in which the heat flow traces (e.g., isothermal or nonisothermal) are simultaneously considered with results of large-scale tests as, e.g., H.1 or H.4 or even ARC. Application of the newly proposed kinetic workflow was proved to increase the accuracy of simulations of SADT based on results collected in the mg-scale and considerably decrease the amount of expensive and time-consuming experiments in kg-scale tests; currently this kinetic approach is included in AKTS Thermal safety software and herein used to reevaluate SAPT from ARC data.

In brief, it is assumed that in small conversion ranges $\Delta\alpha$ the apparent activation energy $E(\alpha)$ and the term $A(\alpha)f(\alpha)$ do not change significantly, so their ratio can be considered as approximatively constant and one can write the following:

$$\ln(A(\alpha)f(\alpha)) \cong CE(\alpha) \quad (7)$$

where C denotes a constant of proportionality. Integration in small α segments yields $E(\alpha)$ values that are practically identical with those obtained by the differential isoconversional analysis, eq 8

$$\frac{d\alpha}{dT_\alpha} = A(\alpha)f(\alpha) \exp\left(\frac{E(\alpha)}{RT_\alpha}\right) \quad (8)$$

which rewritten in logarithmic form gives

$$\ln \frac{d\alpha}{dt_\alpha} = \ln A(\alpha)f(\alpha) - \frac{E(\alpha)}{R} \frac{1}{T(t_\alpha)} \quad (9)$$

and by considering eq 7 leads to the following expression:

$$\ln \frac{d\alpha}{dt_\alpha} \cong E(\alpha) \left(C - \frac{1}{RT(t_\alpha)} \right) \quad (10)$$

After final recombination of eq 7, one obtains the following expression allowing evaluation of the activation energy $E(\alpha)$:

$$E(\alpha) \cong \frac{\ln(d\alpha/dt_\alpha)}{C - \frac{1}{RT(t_\alpha)}} \quad (11)$$

The numerical estimation of the parameter C was done by comparing the reaction progress α of the heat flow signal (e.g., measured at 85 °C for MMA, Figure 12b) and the time of the runaway event in the ARC test, Figure 12a, with their

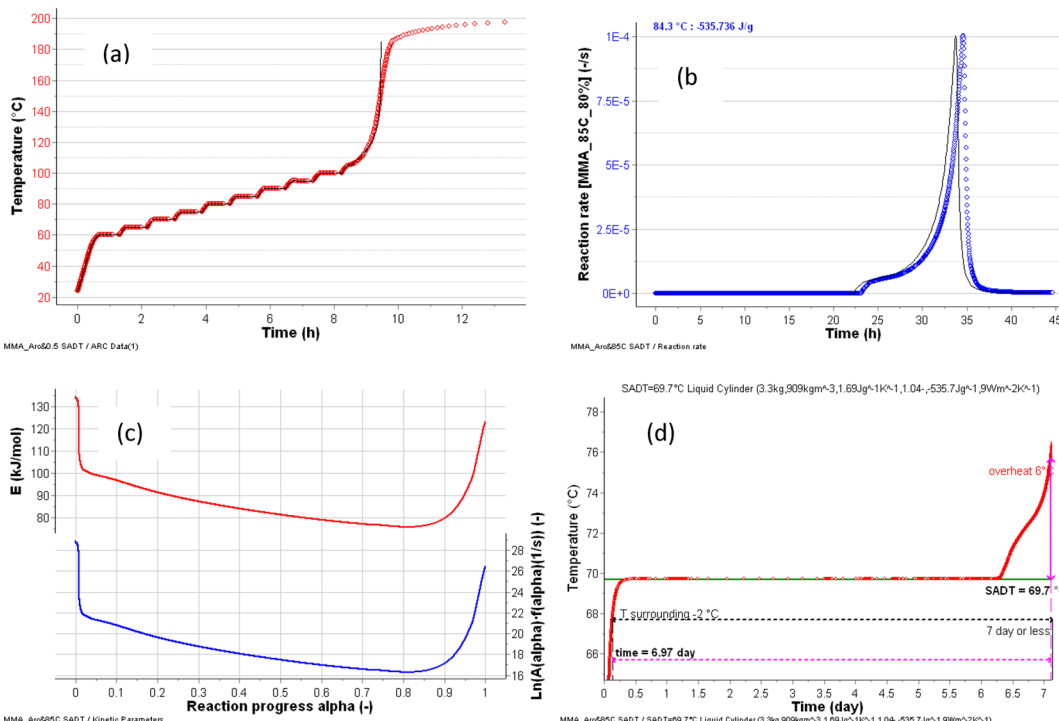


Figure 12. SAPT determination based on merging isothermal calorimetry and ARC data. (a) Measured and fitted ARC data; (b) measured and fitted isothermal calorimetry data; (c) $E(\alpha)$ and $A(\alpha)f(\alpha)$ vs polymerization progress (α); and (d) predicted SADT based on combined data.

simulated courses and using the adequate expression for the heat balance.

The best fit was obtained for the value of $C = 2.15 \times 10^{-4}$ mol/J. Once the optimal value for C is determined, the activation energy $E(\alpha)$ and the term $A(\alpha)f(\alpha)$ can be calculated as a function of the reaction progress using eqs 6 and 10, Figure 12c. The time to runaway of the large-scale test can be then obtained by numerical integration using the suited energy balance equation. As shown in Figure 12d the predicted SADT was 69.7 °C, i.e. about 7.8 °C lower than the value predicted by Semenov's model using the ARC data alone, and more in line with the predictions listed in the last two columns of Table 4.

Using the same Friedman differential isoconversional approach, the SAPT values were calculated from non-isothermal DSC, isothermal calorimetry, and the merging of nonisothermal or isothermal data with the large-scale H1 test. The computed SAPT are summarized in Table 5. It is clear that in spite of the large variation in sample size all methods predict the SAPT for this MMA in a 1 gallon drum within less

than 3 °C, and in good accordance to the SAPT predicted from PIT data (Table 4). Due to a relatively low sample size (normally a couple of mg), high headspace to liquid volume ratio, and challenge to control such a ratio in the DSC test, more work may be needed to confirm that the methods with nonisothermal DSC work for every monomer under every shipping condition. Therefore, the methods with isothermal calorimetry tests are recommended.

3.3. Proposed Methodology for SAPT Evaluation. As defined in UN "Manual of Tests and Criteria",² substances having a SADT greater than 75 °C for a 50 kg package should not be subjected to the classification procedures for self-reactive substances. The heat loss per unit mass for 50 kg packages is in the range 20–100 mW/K/kg². If an H1 test is performed for such 50 kg packages, the heat loss rate with a 6 °C temperature difference at the end of 7 days for the temperature of SAPT will correspond to 120–600 μW/g. The SAPT should be greater than 75 °C when the maximum heat generation rate during the first 7 days in an isothermal PIT measurement at 75 °C is much lower than 120 μW/g. Since the heat generation rate during the induction period of inhibited monomers is normally negligible, it saves further testing and advanced modeling if one can show the PIT measured at 75 °C is well-defined and greater than 7 days with a low maximum heat generation rate. Therefore, a SAPT screening method (a) was proposed, as shown in Figure 13a; when the PIT measured at 75 °C is well-defined and greater than 7 days with the max heat generation rate much lower than 120 μW/g, the SAPT can be reported as greater than 75 °C and then temperature monitoring is not required for the monomer transportation.

For monomers with a well-defined PIT and a low maximum heat generation rate that fail the screening methodology, PIT at 75 °C less than 7 days, SAPT can be estimated based on the Arrhenius-like relationship between PIT and temperature, as

Table 5. Predicted SAPT of 25 ppm MEHQ Inhibited MMA Based on Friedman Differential Isoconversional Kinetics

Method	Mass (g)	C (mol/J)	SAPT (°C)
Isothermal (4 runs at different temperatures)	3.2	—	70.9
Nonisothermal (3 runs at different ramp rates)	0.004–0.007	—	69.2
ARC and Isothermal (85 °C)	4.5	2.15×10^{-4}	69.7
ARC and Nonisothermal (0.5 °C/min)	4.5	2.33×10^{-4}	70.9
H1 and Isothermal (85 °C)	3171	2.36×10^{-4}	72.1
H1 and Nonisothermal (0.5 °C/min)	3171	2.32×10^{-4}	72.1

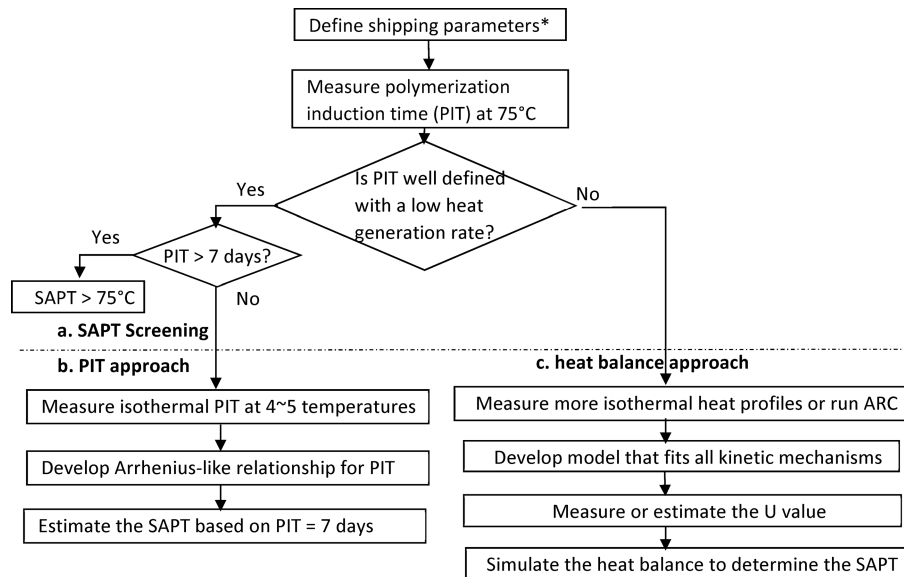


Figure 13. Proposed procedure to determine monomer SAPT for Monomer Transportation Regulation. * The term “shipping parameters” here means the conditions under which the monomer will be shipped, including inhibitor type/concentration, vessel headspace composition, headspace to liquid volume ratio, etc.

discussed in our previous paper. If the PIT is well-defined, the determination of the PIT is less time-consuming than determining heat transfer characteristics of packages and simulating the heat balance of the monomers in the packages. As long as the max heat generation rate during the PIT is much lower than $120 \mu\text{W/g}$, the SAPT estimation based on the temperature at which PIT is equal to 7 days is conservative (PIT approach (b) in Figure 13).

For monomers without a well-defined PIT or having a measurable thermal activity, heat generation, during the PIT, the kinetic parameters for the complete heat profile of a monomer has to be determined from appropriate isothermal calorimetric tests, as discussed. Combining this information with the heat transfer characteristics of the transport container allows for the determination of the SAPT. The determination of SAPT is accomplished by simulating the heat balance for the H1 method and finding the environmental temperature at which the monomer temperature in a package increases from 2°C lower to 6°C higher than the environmental temperature in a period of 7 days (heat balance approach (c) in Figure 13). The determination of the overall heat transfer coefficients in this paper was done under quiescent conditions which is conservative. Under normal shipping conditions, heat removal capabilities are enhanced by wind, increased fluid motions due to jostling of the vessel, and variable ambient temperatures. Therefore, the approach provides a conservative SAPT, and more rigor can be added to estimating heat transfer more accurately if justified because the conservative SAPT results in a significant change in shipping costs. It is worth noting that a more rigorous approach will likely only be warranted when the SAPT value determined by the above approach is only slightly below a trigger temperature for transport (e.g., SAPT under quiescent conditions is $1\text{--}2^\circ\text{C}$ below the cut off temperature requiring the vessel to have active cooling to ship the monomer).

4. CONCLUSIONS

The United Nations Recommendations on the Transport of Dangerous Goods, Model Regulations, Rev.19 (2015) has a new requirement for the determination of the Self-Accelerating Polymerization Temperature (SAPT) for polymerizing substances.

In the previous paper (Part I), the PIT and full kinetics for the methyl methacrylate (MMA) monomer inhibited with 4-methoxyphenol (MEHQ) were determined with isothermal calorimetric tests. In this report, overall heat transfer coefficients of a 1 gallon drum with different chemicals were experimentally determined by measuring the cooling temperature profile and applying both the half-time of cooling method and nonlinear regression method. Film heat transfer coefficient estimation and steady state CFD simulation agree reasonably well with the experimentally obtained values for the overall heat transfer coefficients. Two H1 tests were conducted for a 1 gallon drum with the MMA sample, one at 76°C and another one at 72.2°C . A simulation of both H1 tests using the kinetic model developed from isothermal microcalorimetry and the overall heat transfer coefficients were in good agreement with the actual H1 tests. Specifically, the SAPT determined via simulation agreed well with the SAPT determined by the actual H1 test. The SAPT for MMA with 25 ppm MEHQ in a 1 gallon drum is 71.4°C . In addition, both Semenov’s model and Friedman’s differential isoconversional model were investigated for SAPT estimation.

Finally, a methodology for SAPT evaluation was proposed. According to this methodology, if the PIT of the monomer is greater than 7 days at the lowest allowed SAPT not requiring temperature monitoring (75°C), the SAPT of a commercial package should be greater than this temperature and no additional test should be required. Otherwise, additional testing is needed and SAPT can be estimated based on either the PIT approach or heat balance approach.

AUTHOR INFORMATION

Corresponding Author

*Tel. +01 989-638-2206. E-mail: S25011@hotmail.com.

ORCID

Min Sheng: [0000-0002-5321-2627](https://orcid.org/0000-0002-5321-2627)

Notes

The authors declare no competing financial interest.

ACKNOWLEDGMENTS

The authors thank BAMM, EBAMM, and MPA committees for their suggestions.

NOMENCLATURE

A	surface area (m^2)
A_k	preexponential factor ($1/\text{s}$)
C	reactant concentration (mol/m^3)
C_p	heat capacity ($\text{J}/\text{g}/^\circ\text{C}$)
D	diameter
E_a	activation energy (kJ/mol)
h	convection heat transfer coefficient ($\text{W}/\text{m}^2/^\circ\text{C}$)
ΔH_r	heat of reaction (J/g)
k	thermal conductivity ($\text{W}/\text{m}/^\circ\text{C}$)
m	mass (g)
n	reaction order
Q	total heat
R	universal gas constant ($8.314 \text{ J}/\text{mol}\cdot\text{K}$)
T	temperature ($^\circ\text{C}$)
t	time (s)
U	overall heat transfer coefficient ($\text{W}/\text{m}^2/^\circ\text{C}$)
V	reactant volume (m^3)
α	degree of conversion
β	coefficient of thermal expansion (1/K)
ρ	density (kg/m^3)
μ	viscosity (Pa·s)
g	gravitational acceleration

SUBSCRIPT

$_{\text{o}}$	initial
$_{\text{a}}$	ambient
$_{\text{av}}$	average
$_{\text{i}}$	inside
$_{\text{lm}}$	Log mean
$_{\text{m}}$	Monomer
$_{\text{o}}$	outside
$_{\text{w}}$	wall
$_{\text{z}}$	pseudo-zero-order reaction

REFERENCES

- (1) *UN Recommendations on the Transport of Dangerous Goods, Model Regulations*, 19th revised ed.; United Nations: New York and Geneva, 2015.
- (2) *UN Recommendations on the Transport of Dangerous Goods, Manual of Tests and Criteria*, 5th revised ed.; United Nations: New York and Geneva, 2009.
- (3) Fisher, H. G.; Goetz, D. D. Determination of self-accelerating decomposition temperatures using the Accelerating Rate Calorimeter. *J. Loss Prev. Process Ind.* **1991**, *4* (5), 305–316.
- (4) Kotoyori, T. The self-accelerating decomposition temperature (SADT) of solids of the quasi-autocatalytic decomposition type1. *J. Hazard. Mater.* **1999**, *64* (1), 1–19.
- (5) Lin, W. H.; Wu, S. H.; Shiu, G. Y.; Shieh, S. S.; Shu, C. M. Self-accelerating decomposition temperature (SADT) calculation of methyl ethyl ketone peroxide using an adiabatic calorimeter and model. *J. Therm. Anal. Calorim.* **2009**, *95* (2), 645–651.
- (6) Tseng, J.-M.; Chang, Y.-Y.; Su, T.-S.; Shu, C.-M. Study of thermal decomposition of methyl ethyl ketone peroxide using DSC and simulation. *J. Hazard. Mater.* **2007**, *142* (3), 765–770.
- (7) Liao, C. C.; Wu, S. H.; Su, T. S.; Shyu, M. L.; Shu, C. M. Thermokinetics evaluation and simulations for the polymerization of styrene in the presence of various inhibitor concentrations. *J. Therm. Anal. Calorim.* **2006**, *85* (1), 65–71.
- (8) Cotter, M. A.; Charles, M. E. Transient cooling of petroleum by natural convection in cylindrical storage tanks—II. Effect of heat transfer coefficient, aspect ratio and temperature – Dependent viscosity. *Int. J. Heat Mass Transfer* **1993**, *36*, 2175–2182.
- (9) Fisher, H. G.; Goetz, D. D. Determination of self-accelerating decomposition temperatures for self-reactive substances. *J. Loss Prev. Process Ind.* **1993**, *6* (3), 183–194.
- (10) Cotter, M. A.; Charles, M. E. Transient cooling of petroleum by natural convection in cylindrical storage tanks—I. Development and testing of a numerical simulator. *Int. J. Heat Mass Transfer* **1993**, *36* (8), 2165–2174.
- (11) Ferguson, H. D.; Townsend, D. I.; Hofelich, T. C.; Russell, P. M. Reactive chemicals hazard evaluation: Impact of thermal characteristics of transportation/storage vessel. *J. Hazard. Mater.* **1994**, *37*, 285–302.
- (12) Fernández-Seara, J.; Uhía, F. J.; Dopazo, J. A. Experimental transient natural convection heat transfer from a vertical cylindrical tank. *Appl. Therm. Eng.* **2011**, *31*, 1915–1922.
- (13) Fierz, H. Influence of heat transport mechanisms on transport classification by SADT-measurement as measured by the Dewar-method. *J. Hazard. Mater.* **2003**, *96*, 121–126.
- (14) Steensma, M.; Schuurman, P.; Malow, M.; Krause, U.; Wehrstedt, K.-D. Evaluation of the validity of the UN SADT H.4 test for solid organic peroxides and self-reactive substances. *J. Hazard. Mater.* **2005**, *A117*, 89–102.
- (15) Sheng, M.; Horsch, S.; Dan, F.; Bellair, R.; Holsinger, M.; Weinberg, S.; Sopchik, A. *Calorimetry and Thermo-Kinetic Modeling to Determine SAPT and Safe Shipping Conditions for Self-Reactive Materials*, 2017 Spring Meeting and 13th Global Congress on Process Safety, San Antonio, TX, March 26–29; San Antonio, TX, 2017.
- (16) Hazewinkel, M. *Runge-Kutta Method*; Springer: Berlin, 2001.
- (17) Perry, R. H.; Green, D. W. *Perry's Chemical Engineers' Handbook*; The McGraw-Hill: 1999.
- (18) DIPPR 801 *Policies and Procedures Manual*; Brigham Young University: Provo, UT, 2000.
- (19) Rodríguez, I.; Castro, J.; Pérez-Segarra, C. D.; Oliva, A. Unsteady numerical simulation of the cooling process of vertical storage tanks under laminar natural convection. *Int. J. Therm. Sci.* **2009**, *48* (4), 708–721.
- (20) Mussa, M. A.; Abdullah, S.; Azwadi, C. S. N.; Muhamad, N. Simulation of natural convection heat transfer in an enclosure by the lattice-Boltzmann method. *Comput. Fluids* **2011**, *44* (1), 162–168.
- (21) Heo, J. H.; Chung, B. J. Natural convection heat transfer on the outer surface of inclined cylinders. *Chem. Eng. Sci.* **2012**, *73*, 366–372.
- (22) Neale, A.; Derome, D.; Blocken, B.; Carmeliet, J., Determination of surface convective heat transfer coefficients by CFD. *11th Canadian Conference on Building Science and Technology*, Banff, Alberta, 2007.
- (23) Jayakumar, J. S.; Mahajani, S. M.; Mandal, J. C.; Vijayan, P. K.; Bhoi, R. Experimental and CFD estimation of heat transfer in helically coiled heat exchangers. *Chem. Eng. Res. Des.* **2008**, *86* (3), 221–232.
- (24) Krause, G.; Wehrstedt, K.-D.; Malow, M.; Budde, K.; Mosler, J. Safe Transport of Acrylic Acid in Railroad Tank Cars. Part 1: Determination of the Self-Accelerating Decomposition Temperature. *Chem. Eng. Technol.* **2014**, *37* (9), 1460–1467.
- (25) Singh, S. K. *Self Accelerating Decomposition Temperature (SADT) Determination of Styrene System Using Accelerating Rate Calorimeter*; An ioKinetic, LLC White Paper: 2014.

(26) Dainton, F. S.; Ivin, K. J. Some thermodynamic and kinetic aspects of addition polymerisation. *Q. Rev., Chem. Soc.* **1958**, *12* (1), 61–92.

(27) Roduit, B.; Hartmann, M.; Folly, P.; Sarbach, A.; Brodard, P.; Baltensperger, R. Thermal decomposition of AIBN, Part B: Simulation of SADT value based on DSC results and large scale tests according to conventional and new kinetic merging approach. *Thermochim. Acta* **2015**, *621*, 6–24.